J. Applied Membrane Science & Technology, Vol. 28, No. 2, August 2024, 1–11

Omniphobic PTFE based Hollow Fiber Membrane with ZnO Nanoparticles Deposition via Universal Spray Technique

W. M. Z. Wan Zulkifli[a], M. H. D. Othman[a,b]*, M. A. B. Pauzan[b], N. A. S. M. Hisam[b] & F. H. Jaffar[b]

[a]Department of Energy Engineering, School of Chemical and Energy Engineering, Faculty of Engineering, Universiti Teknologi Malaysia, 81310 UTM Johor Bahru, Johor, Malaysia

[b]Advanced Membrane Technology Research Centre (AMTEC), School of Chemical and Energy Engineering, Faculty of Engineering, Universiti Teknologi Malaysia, 81310 UTM Johor Bahru, Johor, Malaysia

Submitted: 11/1/2024. Revised edition: 28/6/2024. Accepted: 29/6/2024. Available online: 22/7/2024

ABSTRACT

This investigation aimed to enhance the hydrophobicity of a polytetrafluoroethylene (PTFE) hollow fiber membrane, transforming it into an omniphobic surface. This was achieved by coating the membrane with a mixture of zinc oxide nanoparticles (ZnO-NPs) and polyvinylidene fluoride-cohexafluoropropylene (PVDF-HFP) using the universal spray technique. The membrane's morphology and performance were evaluated based on the number of spray cycles, which influenced the coating thickness on the membrane surface. The spraying process was varied up to 4 cycles to determine the membrane with the most effective deposition of ZnO NPs in terms of water contact angle and liquid entry pressure (LEPw). Results indicated that the membrane spray-coated up to 4 cycles, denoted as PTFE-4, exhibited a rough hierarchical re-entrant morphology, imparting omniphobic characteristics. The optimized membrane demonstrated a high water contact angle of 170° and a liquid entry pressure of 2.6 bar. Fourier-transform infrared (FTIR) and energy dispersive analysis of X-rays (EDX) confirmed the successful chemical integration of ZnO NPs onto the commercial membrane. This research holds significance for the future of membrane distillation in treating wastewater containing low surface tension pollutants.

Keywords: Hydrophobic membrane, hollow fiber, nanoparticles, omniphobicity, polymeric membrane

1.0 INTRODUCTION

Every living thing needs clean and safe water to survive, yet as the world's population grows, industrialization progresses, and long-term droughts occur, the demand for safe, clean, and drinkable water grows [1]. Water shortage is a serious problem that affects people all around the world. By 2050, over 6 billion people are anticipated to be affected by water scarcity [2]. Only 3% of the world's water is available for human use, while the remaining 97% is stored as seawater that is unfit for human consumption or agricultural uses [1]. The majority of accessible water is polluted by industrial and agricultural effluents and cannot be drunk without first being treated [3]. Desalination refers to the removal of salt from seawater to produce fresh water suitable for our daily use. Membrane distillation (MD) is a thermally driven separation process, which only allows vapor molecules to

* Corresponding to: M. H. D. Othman (email: hafiz@petroleum.utm.my)
DOI: https://doi.org/10.11113/amst.v28n2.289

pass through a porous hydrophobic membrane and all non-volatile are retained on the retentate side [4]. Vapor pressure differences that exist between the porous hydrophobic membrane surfaces are the driving force for this separation process [5]. The temperature difference across the membrane induces a vapor pressure difference that drives water molecules from the feed to the permeate in the form of vapor[5]. Generally, MD uses an ultrafiltration membrane. The application of MD has many attractive features. For example, a lower operating temperature than multi-stage flash distillation (MSF) and multiple-effect distillation (MED) results, mainly in water not necessarily to heat up to its boiling point for the separation to occur [6]. In addition, reverse osmosis (RO) which is a pressure-driven membrane process experiences a higher hydrostatic pressure than MD with more than 99% salt rejection [5]. MD also has the capability to utilize alternative energy sources such as solar energy and waste energy [7, 8].

Conventional hydrophobic membranes are confined to the treatment of reasonably clean water sources with few surface-active chemicals [9]. Due to the low surface tension pollutants found in wastewater streams, the commercial MD is susceptible to the wetting of the membrane pores. Wetted membrane pores reduce the membrane's effectiveness as a barrier for forming a liquid-vapor interface for fluid streams, limiting MD uses [10]. In a wide range of technical fields, robust omniphobic surfaces that reject both water (hydrophobic) and oil (oleophobic) have gotten a lot of interest [11]. In omniphobic design, re-entrant geometries and specific compositions are needed to achieve excellent wetting resistance to liquids with low surface tension. The desired morphology can be achieved by the deposition of fluorinated nanoparticles (NPs) such as silicon dioxide (SiO_2), titanium dioxide (TiO_2), and zinc oxide (ZnO) on a membrane [12, 13, 11].

For example, an amphiphobic PVDF composite membrane was successfully prepared by dynamically functionalizing perfluorooctyl trichlorosilane (PFTS) and coating the modified SiO_2 nanoparticles onto the membrane surface [12]. The resultant membrane showed anti-fouling and anti-wetting properties against kerosene and humic acid. The liquid entry pressure (LEP) increases significantly from 160 to 250 kPa without compromising the pore size and porosity. The membrane exhibits better permeation stability and anti-fouling towards low surface tension liquid with salt rejection of 99.8% [12]. Next, a microporous PVDF membrane with a hierarchical structure with multilevel surface roughness was created via depositing TiO_2 nanoparticles. The TiO_2-coated membranes were then fluorosilanized using a low surface energy material H, 1H, 2H, 2H-perfluorododecyltrichlorosilane. The resultant membrane showed anti-fouling and anti-wetting properties against glycerol with a surface contact angle increase from 99° to 166° [13]. The total surface roughness of the 1H, 1H, 2H, and 2H-perfluorododecyl-trichlorosilane (FTCS) layer was enhanced as a result of the hierarchical structure in templated coatings, which improved the hydrophobicity [14]. After chemical cleaning of the FTCS–TiO_2–PVDF membrane, a substantial improvement in flux recovery was found, indicating that the membranes' antifouling properties had improved [13]. Interestingly, spherical SiO_2 nanoparticles coating on glass cylindrical fiber manage to give a secondary re-entrant structure resulting in enhanced surface omniphobicity, thus increasing the wetting resistance to low surface tension with a 100 ° contact angle [15]. Another nanoparticle that has been reported by literature that can produce a high surface roughness is ZnO. Due to its outstanding optical, electrical, mechanical, and chemical characteristics, ZnO is one of the most significant multifunctional semiconductor materials, especially for use in photocatalysis and antibacterial compounds. The lower cost of ZnO and the higher surface-to-volume ratio produced when ZnO is employed as nanoparticles make this option a viable method for meeting the demand for a more efficient and low-cost device [16]. In addition, toxicity plays a vital role in nanoparticle application. The use of ZnO does not produce an increase in toxicity due to the size distribution and surface are not related to toxicity. Furthermore, ZnO particles also can produce a wide range of morphologies, including nanowires, nanotubes, nanobelts, nanocombs, and nanospheres using ZnO powder sublimation and deposition [17]. When compared to other nanoparticles such as Ag, Al_2O_3, and TiO_2, ZnO-NPs are also thought to be more cost-effective [18] making them more desirable than any other nanoparticles.

Polymers such as polypropylene (PP), polytetrafluoroethylene (PTFE), polyethylene (PE), and polyvinylidene fluoride (PVDF) are the most common hydrophobic membranes used in MD. PP membrane offers high hydrophobicity and potential higher wetting resistance but due to the low thermal stability the study for this polymer has reduced in the past year [19, 20]. PVDF instead possesses a reasonable wetting resistance, thermal stability, chemical resistance, and mechanical strength but the membrane needs to be modified to suit MD requirements. On the other hand PTFE membrane offers the highest hydrophobicity making it less susceptible to wetting in MD [19]. It also possesses outstanding thermal stability and chemical resistance making it a preferred choice for commercial modules over any other membrane [21], [19]. Plate-and-frame, tubular, spiral-wrapped, and hollow fiber are the four primary types of modules for MD. Due to the high packing density and low energy consumption hollow fiber configuration is more favored than any other configuration for desalination [5]. For surface modification, a variety of methods have been used, including layer-by-layer (LBL), chemical vapor deposition (CVD), and solution blending. However, all these processes need either a long fabrication time or strict operational conditions [22]. Spray coating is another method for surface modification. This compact and environmentally friendly fabrication technique significantly reduces manufacturing time and raw material consumption, resulting in a long-term, scalable, and cost-effective membrane preparation process [16]. Despite these attractive properties, the application of ZnO NPs in fabricating omniphobic polymer hollow fiber membranes using simple and versatile spray coating has not been reported in the literature.

The main objective of this study is to develop omniphobic characteristics on a commercial PTFE hollow fiber membrane by coating the surface of the membrane with Zn NPs using the universal spray coating technique. The Zn NPs will increase the surface roughness of the membrane by developing micro/nanospheres on the membrane which creates the hierarchical re-entrant structure that is responsible for repelling low surface tension liquids. In this study, the commercial PTFE membranes were coated with 4 different cycle numbers in order to find the most effective deposition of Zn NPs on the surface of the membrane The membranes later were characterized by scanning electron microscopy (SEM), energy dispersive analysis of X-rays (EDX), Fourier-transform infrared (FTIR), contact angle and liquid entry pressure.

2.0 METHODS

2.1 Materials

The hydrophobic membrane used as support was purchased from a commercial microfiltration polytetrafluoroethylene (PTFE) hollow fiber membrane. The average pore size provided by the manufacturer is 0.3µm. Meanwhile, for omniphobic layer coating, zinc oxide nanoparticles (ZnO-NPS) (ZnO, Sigma-Aldrich, U.S.A), N, N-Dimethylformamide (DMF, ACROS, Belgium) as solvent, polyvinylidene fluoride-cohexafluoropropylene (PVDF-HFP, Sigma-Aldrich, U.S.A) and 1H, 1H, 2H, (FAS, Aldrich, U.S.A)

2.2 Preparation of Coating Solution

The coating solution was prepared by adding 1.8 g of ZnO-NPS into a total of 200 ml of DMF solvent. To ensure the homogenous dispersion of ZnO, the solution was subjected to a 5 min in an ultrasonic sonicator at the frequency and power of 20 kHz and 80W, respectively. Then, 6 g of PVDF-HFP was added to the homogenous ZnO-DMF solution and vigorously mixed at 65 °C for 12 h on a magnetic stirrer Lastly, 2 ml of FAS was added and mixed for 30 minutes as shown in Figure 1.

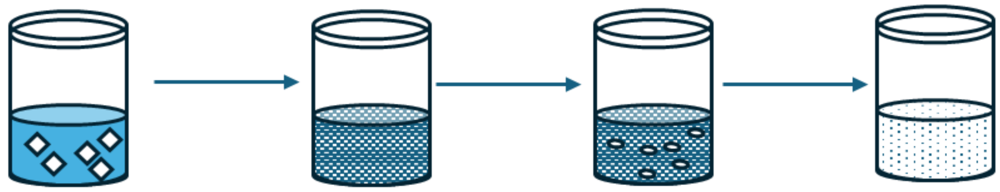

Figure 1 Preparation procedure for the coating solution

2.3 Coating of the Omniphobic Layer onto Polymer Hollow Fiber Membrane

A spray gun (Model: TT-2018) was filled with the omniphobic coating (ZnO/DMF/PVDF-HFP/FAS dope solution). A fixed flow rate of 1.5 mL/h was applied for spray coating. For better coverage of the coating, the hollow fiber membrane was rotated and recorded as a cycle. The PTFE hollow fiber membrane was sprayed for 1 second and dried in the oven (60 °C) for 2 h to complete a cycle as shown in Figure 2 [23]. In this study, 4 membranes namely PTFE-1, PTFE-2, PTFE-3, and PTFE-4 were used where the number at the end of the name represents the number of cycles of each membrane was coated. A pristine membrane with no coating was used as control.

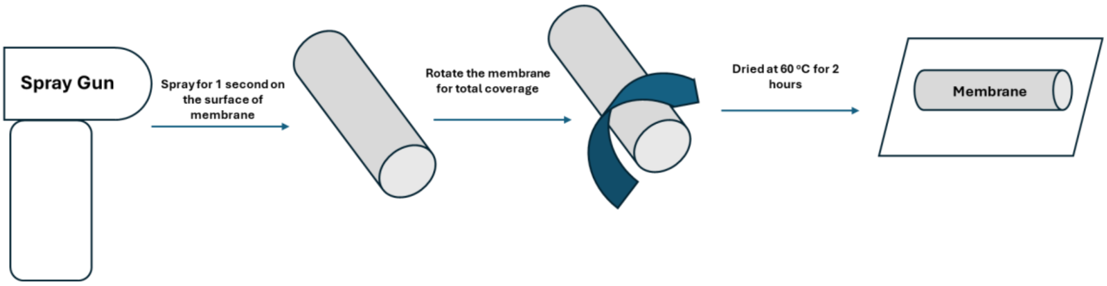

Figure 2 Spray coating procedure onto the commercialized PTFE hollow fiber membrane

2.4 Membrane Characterization

The structural morphology of the membrane's inner and outer were examined qualitatively by scanning electron microscopy (SEM, Model: TM 3000, Hitachi, Japan) and energy dispersion of x-ray (Model: SU8020, Hitachi, Japan). Fourier-transform infrared (FTIR) was used to identify the chemical properties of the modified polymeric membrane. All FTIR spectra were recorded by the attenuated total reflection (ATR) technique using the FTIR spectrometer (Thermoelectron Corporation, Nicolet 5700, U.S.A) at a resolution between 4000 cm^{-1} to 500 cm^{-1}. Contact angle measurements on the membranes were conducted using a contact angle goniometer (Model: OCA 15EC, Dataphysics, Germany) using deionized water. 0.5 μL of water droplets was slowly placed on the membrane surfaces. An average and standard deviation of at least 5 independent measurements were obtained at different spots for each sample. Finally, liquid entry pressure (LEP) was used to determine the wetting resistance of the membranes. The lumen on one side of the membrane was blocked by epoxy resin. Then, the adapter holding the membrane was inserted into the module. Compressed carbon dioxide was used to push the water to penetrate the membrane. The pressure was increased by 0.1 bar for 10 seconds until the first drop of water was seen dripping from the membrane.

3.0 RESULTS AND DISCUSSION

3.1 Morphology

Figure 3 presents the SEM images illustrating the different surface morphologies due to the different cycles of the omniphobic coating. The SEM images of the uncoated commercial PTFE hollow fiber pristine membrane used as the control are presented in Figure 3A (1-2). The pore sizes of the coated membranes have reduced as the number of cycles increased due to the presence of Zn NPS. Even though the PTFE-1 was sprayed with the same type of coating solution, they did not exhibit the desired morphology for omniphobic as there was no formation of a spherical microsphere on the surface of the membrane as illustrated in Figure 3 B (1-2). This is due to the lack of dispersion of Zn NPs on the surface of the membrane. By increasing the number of spray coating cycles, the spherical microspheres comprised of ZnO had created the hierarchical micro/nano re-entrant surface morphology as portrayed in Figure 3C up to Figure 3E. It was visible from SEM images of all three samples that the formation of web-like structures increased the number of microspheres on the surface of membranes. Hence, the surface morphology of the PTFE-3 and PTFE-4 matched the hillock valley style of re-entrant structures which are responsible for the repellence of low surface tension liquids [11].

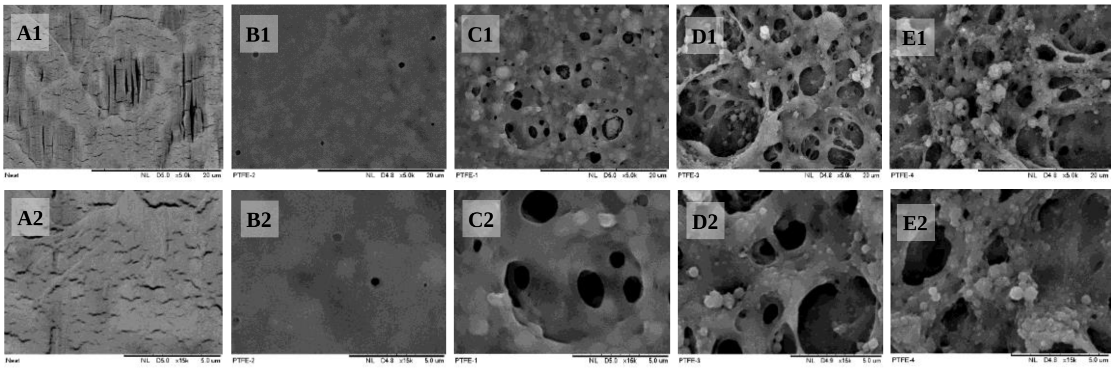

Figure 3 SEM images at 5k and 15k magnifications of the (A) Pristine, (B) PTFE-1, (C) PTFE-2, (D) PTFE-3, (E) PTFE-4 membranes

3.2 Element Distribution

Energy dispersive analysis of X-rays (EDX) was performed to detect the presence of Zn NPs on the surface of the membranes. Based on Figure 4, by using the spray method, Zn NPs were effectively deposited on the surface of the membrane. The blue dot in the figure represents the Zn distribution on the membrane. The distribution of Zn NPs on the surface of PTFE-1 to PTFE-3 membranes was not uniform. This results in a gap for low surface tension liquid to seep into the membrane making it more susceptible to membrane wetting. However, PTFE-4 portrayed the most uniform distribution and the highest concentration of Zn NPs on its surface making it the most efficient out of other coated membranes.

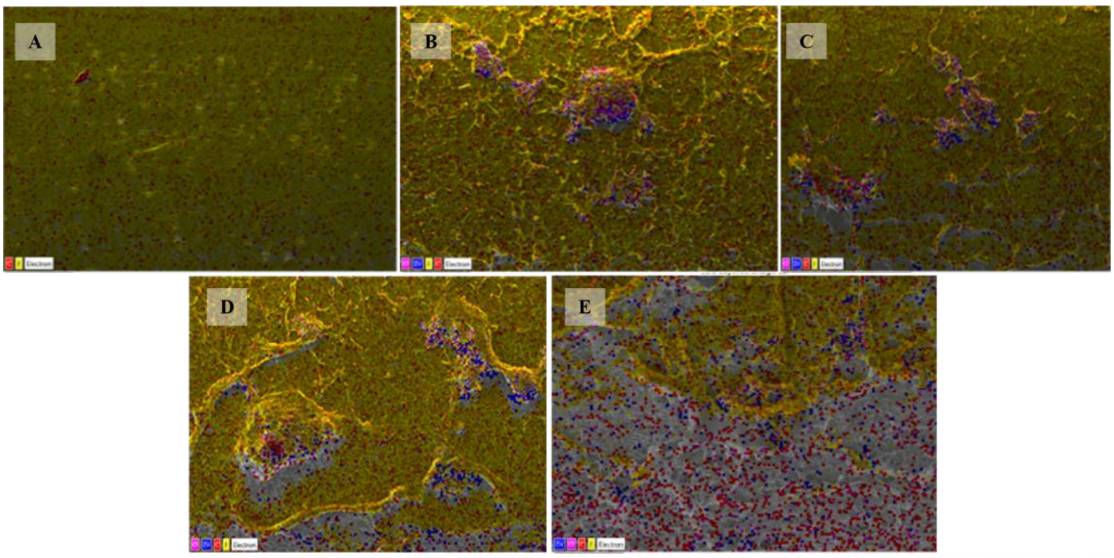

Figure 4 EDX images of the (A) Pristine, (B) PTFE-1, (C) PTFE-2, (D) PTFE-3 and (E) PTFE-4 surfaces

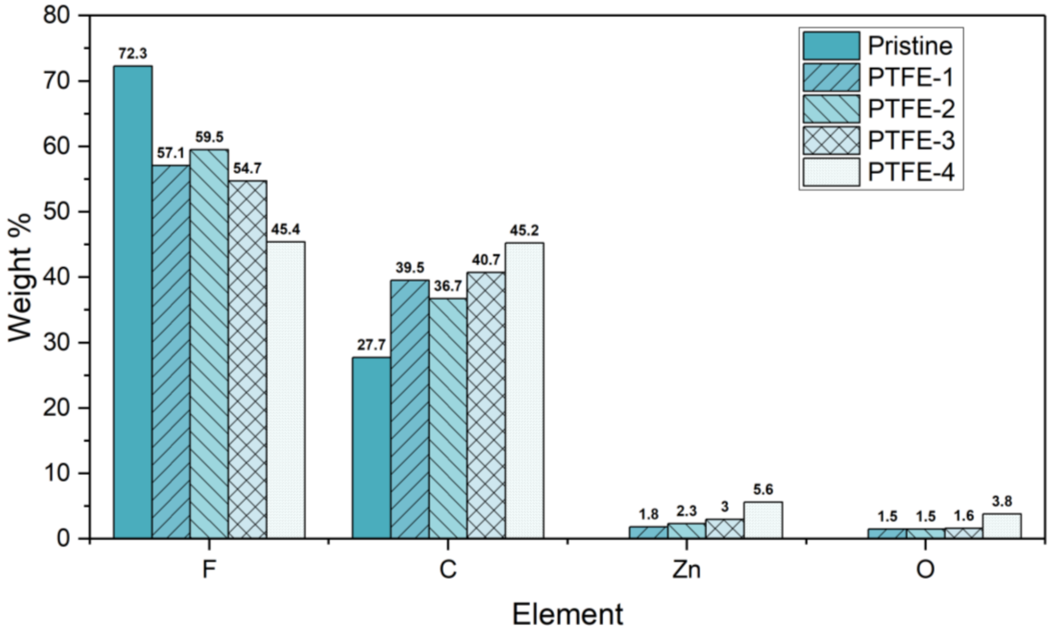

Figure 5 Elemental composition of membranes

3.3 Functional Groups

Figure 6 depicts the FTIR spectra of all membranes. The infrared absorption spectra of the coated membrane show several new absorption peaks compared to the pristine membrane. The new peaks 1(533.81 cm^{-1}) to 2(638.06 cm^{-1}) indicated the presence of the ZnO NPs on the membrane surface which corresponded to a previous study by Suresh *et al.*, 2018 [24]. Peaks 6 and 7 represent the characteristic peaks for C−F i.e., 1200.94 cm^{-1} (symmetric C−F stretch), 1147.45 cm^{-1} (asymmetric C−F stretch) [25]. The β-phase, amorphous phase, and α-phase of the PVDF-HFP can be seen at peaks 3-5 with bands at 837.43 cm^{-1}, 876.0 cm^{-1}, and 1070.43 cm^{-1} respectively [25,26]. Lastly, peaks 8 (1401.47 cm^{-1}) are assigned to -CH_2 bending.

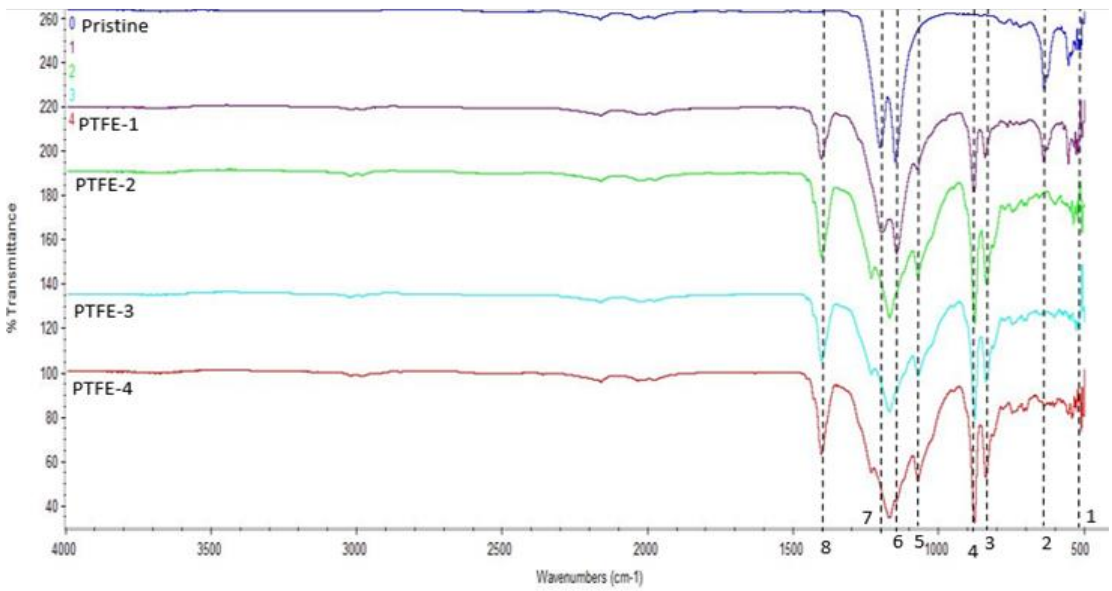

Figure 6 FTIR spectra of the membranes

3.4 Contact Angle

The water contact angle of the coated PTFE hollow fiber membranes has increased proportionally to the number of spray cycles ranging from (123.0 ± 3.2°) to 170° as shown in Figure 7. This is due to the dispersion of the ZnO nanoparticles on the surface of the membranes has increased the surface roughness of the membrane. This desired result is portrayed by the PTFE-4 membrane as shown in Figure 3 which exhibits the highest water contact angle of 170°. Similar observations were made by Deka *et al.*, 2019 as their fabricated membrane with omniphobic characteristics showed an increase of water contact angle from (125.8 ± 3.0°) to (152.2 ± 3.1°) by coating them with the same coating solution [11].

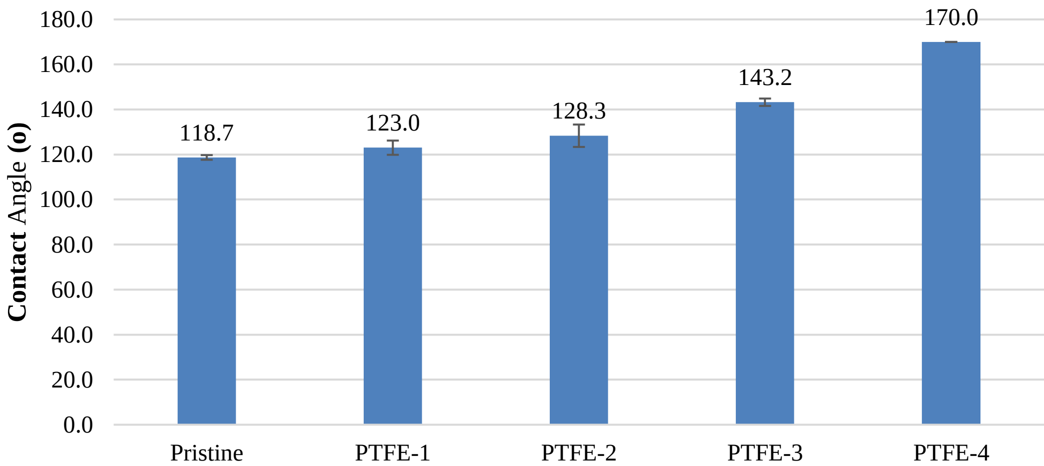

Figure 7 Water contact angle of membranes at average 5 samples per membrane

3.5 Liquid Entry Pressure (LEP)

The LEP values of the membranes were measured to determine the wetting resistance of the membranes. The coated membrane showed an increase in LEP value from the pristine membrane. The data obtained was in agreement with previous work by Lu *et al*., 2016 [12] where the increase in LEP values from 1.6 to 2.5 bar for the membrane coated with NPs. When a coating layer is added to a membrane, it can increase the roughness of the membrane surface as portrayed in SEM images (Figure 3). This increase in roughness can lead to the formation of air gaps within the membrane structure, affecting its wetting properties and overall performance. The relationship between membrane roughness and the creation of an air gap, as explained by the Cassie-Baxter model, is a critical aspect of understanding the behavior of coated membranes. Based on Figure 8, the LEP value of the membrane increased proportionally to the number of cycles due to the increased concentration of Zn NPs on the surface of the membranes. However, only the LEP value of PTFE-4 was above the recommended minimum value for MD membrane which is 2.5 bar making it the most suitable for MD [26]. Metya *et al.* [29] observed a linear relation between roughness and interfacial tension in Cassie-Baxter and Wenzel states, suggesting increased roughness alters wetting behavior and liquid entry pressure. Therefore, the high LEP value is due to the high hydrophobicity exhibited by the membrane resulting from the rough surface of the membrane.

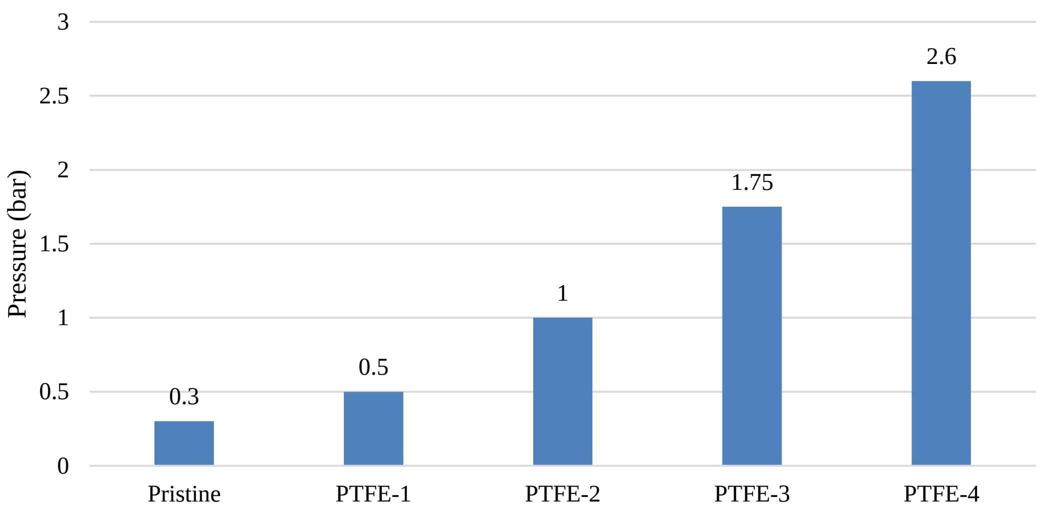

Figure 8 Water contact angle of membranes at average 5 samples per membrane

4.0 CONCLUSION

This study illustrated the successful deposition of Zn NPs by spray coating technique with ZnO NPS with PVDF-HFP on the surface of commercialized PTFE hollow fiber membrane. The presence of Zn NPs on the surface of the membrane has developed an omniphobic characteristic due to the formation of spherical microspheres comprised of ZnO that creates the hierarchical micro/nano re-entrant surface morphology. The fabricated membrane, PTFE-4 was found to possess the highest contact angle at 170° and LEP at 2.6 than the other coated membranes making it the most optimal membrane. The FTIR and EDX evidenced the chemical integration of the ZnO NPs with the commercialized membrane. To conclude, this work revealed a methodology to produce omniphobic characteristics in commercial membranes using organosilane functionalization and surface fluorination with ZnO NPs via the easy and adaptable process of spraying technique. This successfully improved the membrane's ability to handle low surface tension liquids, allowing MD technology to be used in more applications.

ACKNOWLEDGEMENT

The authors gratefully acknowledge the financial support from the Universiti Teknologi Malaysia for the research funding under the Zamalah Grant (Project Number: Q.J130000.7709.00N01) and Fundamental Research (Project Number: Q.J130000.3809.22H07).

CONFLICTS OF INTEREST

The authors declare that there is no conflict of interest regarding the publication of this paper.

REFERENCES

[1] C. Santhosh, V. Velmurugan, G. Jacob, S. K. Jeong, A. N. Grace, A. Bhatnagar. (2016). Role of nanomaterials in water treatment applications: A review. *Chemical Engineering Journal, 306,* 1116-1137.

[2] A. Boretti, L. Rosa. (2019). Reassessing the projections of the World Water Development Report. *NPJ Clean Water, 2.*

[3] D. T. Moussa, M. H. El-Naas, M. Nasser, M. J. Al-Marri. (2017). A comprehensive review of electrocoagulation for water treatment: Potentials and challenges. *J Environ Manage, 186*, 24-41.

[4] E. Drioli, A. Ali, F. Macedonio. (2015). Membrane distillation: Recent developments and perspectives. *Desalination, 356*, 56-84.

[5] A. Alkhudhiri, N. Darwish, N. Hilal. (2012). Membrane distillation: A comprehensive review. *Desalination*, *287*, 2-18.

[6] U. K. Kesieme, N. Milne, H. Aral, C. Y. Cheng, M. Duke. (2013). Economic analysis of desalination technologies in the context of carbon pricing, and opportunities for membrane distillation. *Desalination, 323*, 66-74.

[7] J. Blanco Gálvez, L. García-Rodríguez, I. Martín-Mateos. (2009). Seawater desalination by an innovative solar-powered membrane distillation system: the MEDESOL project. *Desalination*, *246*, 567-576.

[8] M. Khayet. (2013). Treatment of radioactive wastewater solutions by direct contact membrane distillation using surface modified membranes. *Desalination*, *321*, 60-66.

[9] S. Lin, S. Nejati, C. Boo, Y. Hu, C.O. Osuji, M. Elimelech, (2014). Omniphobic membrane for robust membrane distillation. *Environ Sci Technol Lett., 1*, 443-447.

[10] S. Mosadegh-Sedghi, D. Rodrigue, J. Brisson, M. C. Iliuta. (2014). Wetting phenomenon in membrane contactors - Causes and prevention. *J Memb Sci., 452*, 332-353.

[11] B. J. Deka, J. Guo, N. K. Khanzada, A. K. An. (2019). Omniphobic re-entrant PVDF membrane with ZnO nanoparticles composite for desalination of low surface tension oily seawater. *Water Res., 165*, 114982.

[12] X. Lu, Y. Peng, L. Ge, R. Lin, Z. Zhu, S. Liu. (2016). Amphiphobic PVDF composite membranes for anti-fouling direct contact membrane distillation. *J Memb Sci., 505*, 61-69.

[13] A. Razmjou, E. Arifin, G. Dong, J. Mansouri, V. Chen. (2012). Superhydrophobic modification of TiO_2 nanocomposite PVDF membranes for applications in membrane distillation. *J Memb Sci.,* 415-416, 850-863.

[14] S. Meng, J. Mansouri, Y. Ye, V. Chen. (2014). Effect of templating agents on the properties and membrane distillation performance of TiO_2-coated PVDF membranes. *J Memb Sci., 450*, 48-59.

[15] C. Boo, J. Lee, M. Elimelech. (2016). Engineering surface energy and nanostructure of microporous films for expanded membrane distillation applications. *Environ Sci Technol., 50*, 8112-8119.

[16] S. Balta, A. Sotto, P. Luis, L. Benea, B. van der Bruggen, J. Kim. (2012). A new outlook on membrane enhancement with nanoparticles: The alternative of ZnO. *J Memb Sci., 389*, 155-161.

[17] Z. L. Wang. (2007). Novel nanostructures of ZnO for nanoscale photonics, optoelectronics, piezoelectricity, and sensing. *Appl Phys A Mater Sci Process., 88*, 7-15.

[18] S. Liang, K. Xiao, Y. Mo, X. Huang. (2012). A novel ZnO

nanoparticle blended polyvinylidene fluoride membrane for anti-irreversible fouling. *J Memb Sci.,* 394-395, 184-192.

[19] N. Thomas, M. O. Mavukkandy, S. Loutatidou, H. A. Arafat. (2017). Membrane distillation research & implementation: Lessons from the past five decades. *Sep Purif Technol., 189*, 108-127.

[20] L. Eykens, K. de Sitter, C. Dotremont, L. Pinoy, B. van der Bruggen. (2016). How to optimize the membrane properties for membrane distillation: A review. *Ind Eng Chem Res., 55*, 9333-9343.

[21] Z. S. Tai, M. H. A. Aziz, M. H. D. Othman, A. F. Ismail, M. A. Rahman, J. Jaafar. 2019. An overview of membrane distillation. *Membrane separation principles and applications*. Elsevier.

[22] S. S. Ray, S. S. Chen, C. W. Li, N. C. Nguyen, H. T. Nguyen. (2016). A comprehensive review: Electrospinning technique for fabrication and surface modification of membranes for water treatment application. *RSC Adv., 6*, 85495-85514.

[23] M. H. Abd Aziz, M. A. B. Pauzan, N. A. S. Mohd Hisam, M. H. D. Othman, M. R. Adam, Y. Iwamoto, M. Hafiz Puteh, M. A. Rahman, J. Jaafar, A. Fauzi Ismail, T. Agustiono Kurniawan, S. Abu Bakar. (2022). Superhydrophobic ball clay-based ceramic hollow fiber membrane via universal spray coating method for membrane distillation. *Sep Purif Technol., 288*, 120574.

[24] J. Suresh, G. Pradheesh, V. Alexramani, M. Sundrarajan, S.I. Hong. (2018). Green synthesis and characterization of zinc oxide nanoparticle using insulin plant (Costus pictus D. Don) and investigation of its antimicrobial as well as anticancer activities. *Advances in Natural Sciences: Nanoscience and Nanotechnology,* 9.

[25] J. Hubert, T. Dufour, N. Vandencasteele, S. Desbief, R. Lazzaroni, F. Reniers. (2012). Etching processes of polytetrafluoroethylene surfaces exposed to He and He-O_2 atmospheric post-discharges. *Langmuir, 28*, 9466-9474.

[26] Q. Meng, W. Li, Y. Zheng, Z. Zhang. (2010). Effect of poly(methyl methacrylate) addition on the dielectric and energy storage properties of poly(vinylidene fluoride). *J Appl Polym Sci., 116*, 2674-2684.

[27] G. Peng, X. Zhao, Z. Zhan, S. Ci, Q. Wang, Y. Liang, M. Zhao. (2014). New crystal structure and discharge efficiency of poly(vinylidene fluoride-hexafluoropropylene)/poly(methyl methacrylate) blend films. *RSC Adv., 4*, 16849-16854.

[28] K. Schneider, W. Holz, R. Wollbeck, S. Ripperger. 1988. Membranes and modules for transmembrane distillation. *Journal of Membrane Science, 39*(1), 25-42.

[29] A. K. Metya, S. Khan, J. K. Singh. (2014). Wetting transition of the ethanol–water droplet on smooth and textured surfaces. *The Journal of Physical Chemistry C, 118*, 4113-4121.